NACA

RESEARCH MEMORANDUM

TRANSONIC FLUTTER INVESTIGATION OF A 64° DELTA WING CONSTRUCTED WITH SPARS ALONG CONSTANT-PERCENT CHORD LINES AND STREAMWISE RIBS

By George W. Jones, Jr.

Langley Aeronautical Laboratory
Langley Field, Va.

NATIONAL ADVISORY COMMITTEE
FOR AERONAUTICS

WASHINGTON
August 12, 1957

X

NATIONAL ADVISORY COMMITTEE FOR AERONAUTICS

RESEARCH MEMORANDUM

TRANSONIC FLUTTER INVESTIGATION OF A 64° DELTA WING CONSTRUCTED WITH SPARS ALONG CONSTANT-PERCENT CHORD LINES AND STREAMWISE RIBS

By George W. Jones, Jr.

SUMMARY

An experimental investigation has been made in the Langley transonic blowdown tunnel of the transonic flutter characteristics of a 64° delta wing which simulated in a crude manner a construction having spars along constant-percent chord lines and streamwise ribs. The data obtained were compared with previously published data on a 64° delta wing with construction which simulated spanwise spars and orthogonal streamwise ribs.

Results for the present wing agreed with those for the wing with spanwise spars and streamwise ribs in that about the same flutter characteristics were exhibited from Mach numbers of 0.79 to 0.96 and also a sharp increase occurred at Mach numbers above 0.96 in the value of the parameter consisting of flutter-speed coefficient divided by the square root of mass density ratio. Within the operating limits of the tunnel the present wing, however, could not be fluttered above a Mach number of 0.96 even though values of the parameter, flutter-speed coefficient divided by the square root of mass density ratio, exceeded by as much as 10 percent those required to flutter the wing with spanwise spars and streamwise ribs.

INTRODUCTION

Only limited data are available on the transonic flutter characteristics of delta plan-form wings (see, for instance ref. 1). Two exploratory investigations have accordingly been made in the Langley transonic blowdown tunnel in an attempt to define some of the transonic flutter problems of delta wings. In the first of the two investigations transonic flutter tests were made on a 64° delta wing in which the wing was made to simulate in a crude manner one general type of wing construction, namely spars normal to the fuselage plane of symmetry and streamwise ribs.

[redacted]

The results of the first investigation were published in reference 2. The second investigation consisted of transonic flutter tests on a 64° delta wing which was built so as to simulate another type of construction, which consists of spars along constant-percent chord lines and streamwise ribs.

The present paper reports on the second investigation. In the tests an attempt was made to flutter the wing over a Mach number range from 0.69 to 1.31. The model was cantilever mounted at zero angle of attack without body freedoms.

SYMBOLS

b	streamwise strip semichord measured along chordwise center line of strip, ft
b_r	reference wing streamwise semichord, mean geometric exposed semichord, ft
f_i	measured coupled natural frequencies (i = 1, 2, or 3), cps
f_α	measured coupled predominantly torsion natural frequency, f_3, cps
g_h	structural damping coefficient in bending
$I_\alpha \delta$	mass moment of inertia of streamwise wing strip of width δ about a spanwise axis passing through the strip center-of-gravity position, slugs-ft^2
M_e	experimental Mach number
$m\delta$	mass of a streamwise wing strip of width δ, slugs
q_e	experimental dynamic pressure, $\frac{\rho_e V_e^2}{2}$, lb/sq ft
t/c	ratio of wing thickness to streamwise chord
V_e	experimental free-stream velocity, ft/sec
x_{cg}	streamwise distance from leading edge to center-of-gravity position of streamwise strip, fraction of streamwise chord
δ	width of streamwise wing strip, ft

η nondimensional distance along exposed wing span, $\frac{\text{Spanwise distance measured from wing root}}{\text{Length of exposed span}}$

μ_e experimental mass density ratio, $\frac{\text{Exposed panel mass}}{(\text{Exposed panel span})(\pi\rho_e b_r^2)}$

Λ sweepback angle of leading edge, deg

ρ_e experimental free-stream air density, slugs/cu ft

ω_e measured angular frequency of flutter, radians/sec

ω_i angular coupled natural frequencies, $2\pi f_i$, radians/sec

ω_α angular coupled predominantly torsion natural frequency, ω_3, radians/sec

MODELS

Configuration

A sketch of the delta wing showing the basic dimensions and construction is given in figure 1 and some of the wing geometric parameters are listed in table I(a). The leading-edge sweepback angle was 64° and the tips were clipped along streamwise lines. The streamwise wing sections had a rounded leading edge over approximately 4 percent chord, straight parallel top and bottom surfaces to 85 percent chord, and a straight taper top and bottom from 85 percent chord to a sharp trailing edge. Along the span the wing had a nearly constant ratio of thickness to chord of 1.25 percent except that near the tip the thickness ratio increased somewhat. (See fig. 2.)

Construction

The delta-wing test model was constructed from a blank of 2024 aluminum alloy which was formed into two wing panels, each shaped as described in the previous section, and an integral mounting block shown in figure 1. One of the two solid panels was modified to simulate rib and spar construction by cutting away the metal in order to leave a pattern of streamwise ribs and spars along constant-percent chord lines as shown in figure 1. The cut-outs were filled with a lightweight low-stiffness foam plastic and the entire panel was wrapped with a sheet of 0.003-inch-thick Fiberglas which was glued in place with a polyester resin.

Physical Parameters

Some of the wing physical properties are given in table I. The structural damping coefficient (table I(a)) was determined from the decrement of free-bending vibrations in still air. The frequencies (table I(a)) and node lines which are presented in figure 3 were measured by use of an electromagnetic shaker mounted close to the wing root. (See fig. 3.) Salt crystals sprinkled on the wing while vibrating depicted the node lines at the natural frequencies.

After testing, the exposed modified panel was cut into five streamwise strips. The mass, the center-of-gravity location, and the mass moment of inertia about a spanwise axis through the center of gravity were determined for each strip (table I(b)). The methods used to determine these parameters are discussed in reference 3. The division of the panel into strips, the strip center-of-gravity locations, and the assumed strip axes for measurement of moment of inertia are shown in figure 4.

APPARATUS AND TESTS

A detailed description of the tunnel, the model mount, the instrumentation, and the testing technique is given in reference 3; therefore, only a brief description of these items is given in the following paragraphs.

The flutter tests were made in the Langley transonic blowdown tunnel, a slotted tunnel with an octagonal test section which measures 26 inches between flats. Excellent agreement between flutter data obtained in the tunnel and in free air is shown in reference 4. In operating the tunnel, a preselected Mach number is set by means of a variable orifice downstream of the test section and this Mach number is held approximately constant (after the orifice is choked) while the stagnation pressure, and thus density, is increased until flutter is obtained. The tunnel can operate from subsonic Mach numbers through the transonic range and up to a supersonic Mach number of about 1.4. The density range is approximately 0.001 to 0.012 slug per cubic foot. It should be noted that because of the expansion of the air in the reservoir during a run the stagnation temperature continually decreases so that the test-section velocity is not uniquely defined by the Mach number. Mach number is a function of temperature and there is no independent control of the temperature.

The test wing was mounted at zero angle of attack in a cylindrical sting fuselage which extends upstream without change in diameter into the subsonic flow region of the tunnel. Thus, the formation of a bow shock wave which might reflect from the tunnel walls onto the model is prevented.

The weight of the model support system is 289 pounds and the fundamental frequency of the system is approximately 15 cycles per second.

The model instrumentation consisted of wire strain gages mounted on the wing as shown in figure 3 and oriented in order to indicate deflections of the wing panel about two different axes. A recording oscillograph was used to obtain a continuous record during each run of the strain-gage signals and of stagnation temperature, stagnation pressure, and test-section static pressure. The record of the strain-gage signals was used to determine the start of flutter and the frequency of the wing oscillations.

The Mach number range over which flutter was obtained on the wing was from 0.69 to 0.96, but attempts were made to flutter the wing at Mach numbers up to 1.3 and dynamic pressures up to 4,158 pounds per square foot.

RESULTS

General Comments

For each of the flutter points, only the modified wing panel fluttered. The other panel of solid 2024 aluminum was too stiff to flutter in the density range of the tunnel.

Approximately half of the flutter points were readily determined from the oscillograph strain-gage records. These starts of flutter were characterized by a change from random wing motion to a continuous sinusoidal oscillation accompanied by an increase in oscillation amplitude. Also the oscillation frequencies of both strain-gage traces became the same at the start of flutter. For the other half of the flutter points a period of intermittent sinusoidal oscillations preceded the start of flutter and obscured the exact start of flutter. Such periods are designated as low-damping regions inasmuch as the sum of the aerodynamic and structural damping is close to zero and the wing has a large response to random disturbances such as tunnel turbulence. When low damping occurred, two data points were picked - one near the start of the low-damping region and the other near the start of continuous flutter following low damping. Both data points are presented in the tables and figures.

The operating characteristics of the tunnel were such that during a single run the tunnel operating curve of dynamic pressure as a function of Mach number sometimes intersected at two points the model flutter-boundary curve of dynamic pressure required for flutter as a function of Mach number. In such cases both points of intersection are presented in the data.

Presentation of Data

The results of the tunnel tests are listed in table II. The first three columns describe chronologically the flutter behavior of the test wing panel during each tunnel run. The first column gives the tunnel run number, the second column lists in chronological order the data points of interest during each run, and the third column, by means of code letters (defined in table II), describes the behavior of the wing at each data point. The remaining columns give information about each data point such as flutter Mach number and frequency, dynamic pressure, velocity, and so forth.

Some of the results tabulated in table II are presented as functions of Mach number in figures 5 to 8. Figure 5 is a plot of dynamic pressure at flutter; figure 6 is a plot of the parameter $\frac{V_e}{b_r \omega_\alpha \sqrt{\mu_e}}$ at flutter; figure 7 is a comparison of values of the parameter $\frac{V_e}{b_r \omega_\alpha \sqrt{\mu_e}}$ for the test wing with the values of the same parameter for wing 1 of reference 2; and figure 8 is a plot of the flutter frequency normalized by the third natural coupled frequency which is designated as the predominantly torsion frequency. In figures 5, 6, and 7 the low-damping regions are indicated by dashed lines which extend from the start-of-low-damping point (marked only by the lower end of the dashed line) to the continuous-flutter point (marked by a symbol at the upper end of the dashed line).

DISCUSSION

The flutter tests on the present wing were made over a Mach number range from 0.69 to 1.31, and flutter was obtained at Mach numbers from 0.69 to 0.96. The flutter boundary obtained is plotted in figure 5 as dynamic pressure required for flutter against Mach number and shows a dip around Mach number 0.8 followed by a rise between Mach numbers 0.9 and 0.96. The flutter frequencies obtained (table II) fell between the frequencies of the first two coupled modes (fig. 3).

Three runs were made at Mach numbers between 0.96 and 1.31 and no flutter was obtained although approximately maximum tunnel dynamic pressure was reached. The variations of test-section dynamic pressure with Mach number during these runs are shown in figure 5 by short-dashed—long-dashed lines with solid points at the upper end of the lines which indicate the maximum dynamic pressure reached. Although no flutter occurred during these runs, considerable response of the wing to random disturbances was noted. The no-flutter lines and points in figure 5 show that the dynamic pressure required for flutter of the present wing must increase by a factor of about 2.5 between Mach numbers 0.96 and 1.05.

[redacted]

In figure 6 the data for the present wing are shown in the form of the more general nondimensional parameter $\frac{V_e}{b_r\omega_\alpha\sqrt{\mu_e}}$ which consists of the flutter-speed coefficient divided by the square root of the mass ratio. Between the Mach numbers 0.69 and 0.96, the values of $\frac{V_e}{b_r\omega_\alpha\sqrt{\mu_e}}$ varied from 0.33 to 0.38 with a dip around Mach number 0.8 followed by a rise between Mach numbers 0.90 and 0.96. The points for maximum dynamic pressure, no-flutter show that, if a flutter boundary exists at supersonic Mach numbers, the values of $\frac{V_e}{b_r\omega_\alpha\sqrt{\mu_e}}$ must rise from 0.38 to some value above 0.59 between Mach numbers of 0.96 and 1.05.

As mentioned in the "Introduction" this is the second transonic flutter investigation made on a 64° delta wing in the Langley transonic blow-down tunnel. Wing 1 of reference 2 was externally similar to the present wing but had a construction which simulated spars normal to the fuselage plane of symmetry and orthogonal streamwise ribs. The vibration node lines for both wings were quite similar. A comparison of frequency data for the two wings is given in the following table:

	Present wing (spars along constant-percent chord lines)	Wing 1 of reference 2 (spanwise spars and orthogonal, streamwise ribs)
f_1, cps . . .	120	108
f_2, cps . . .	274	253
f_3, cps . . .	438	342
f_1/f_3	0.27	0.32
f_2/f_3	0.63	0.74

The frequencies of the present wing are higher than those for wing 1 of reference 2, but the frequency ratios f_1/f_3 and f_2/f_3 for the present wing are only slightly lower than the corresponding ratios for wing 1 of reference 2.

The parameter $\frac{V_e}{b_r\omega_\alpha\sqrt{\mu_e}}$ is used in figure 7 to compare the flutter behavior of the present wing with that of wing 1 of reference 2. Between

Mach numbers 0.79 and 0.96 where the data for the two wings overlap, the values of $\frac{V_e}{b_r\omega_\alpha\sqrt{\mu_e}}$ for the two wings are nearly the same. In reference 2 the parameter $\frac{V_e}{b_r\omega_\alpha\sqrt{\mu_e}}$ was shown to correlate at a given Mach number the data for two different wings having the same plan form and general type of construction but different masses and frequencies. The present wing and wing 1 of reference 2 have different types of construction but the plan forms are the same and the frequency ratios are similar. Therefore, it is thought that the aforementioned agreement of $\frac{V_e}{b_r\omega_\alpha\sqrt{\mu_e}}$ values between the present wing and wing 1 of reference 2 is an indication that the flutter modes for the two wings in this Mach number range were quite similar. Additional evidence of the similarity of the flutter modes for the two wings is given in figure 8 which shows the ratio of flutter frequency to torsion frequency for the present wing to be around 0.5 with scatter from 0.45 to 0.57. These values are nearly the same as those for wing 1 of reference 2 in the same Mach number range. Thus the differences in construction between the two wings appear to have little effect on the values of $\frac{V_e}{b_r\omega_\alpha\sqrt{\mu_e}}$ and $\frac{\omega_e}{\omega_\alpha}$ for the two wings in the Mach number range from 0.79 to 0.96.

For wing 1 of reference 2 a large and abrupt increase in $\frac{V_e}{b_r\omega_\alpha\sqrt{\mu_e}}$ values occurred at about Mach number 1.05 and flutter at this higher level was encountered at Mach numbers up to 1.28. (See fig. 7.) This abrupt increase in $\frac{V_e}{b_r\omega_\alpha\sqrt{\mu_e}}$ values was accompanied by an abrupt increase in the ratio of flutter frequency to torsion frequency. As discussed in reference 2, these phenomena were interpreted as evidence of an abrupt change in flutter mode from a low-frequency to a high-frequency flutter mode. Abrupt changes in flutter mode have been noted before. (See refs. 1 and 5.) The present wing did not flutter at Mach numbers from 0.96 to 1.3 although, in this range, the wing was tested to higher values of $\frac{V_e}{b_r\omega_\alpha\sqrt{\mu_e}}$ than were needed to flutter wing 1 of reference 2. These no-flutter points are shown in figure 7. The subsonic flutter points and supersonic no-flutter points shown for the present wing in figure 7 indicate that a sharp rise in $\frac{V_e}{b_r\omega_\alpha\sqrt{\mu_e}}$ occurred for this wing between Mach numbers 0.96 and 1.05.

CONCLUSIONS

From a transonic flutter investigation of a 64° delta wing constructed with spars along constant-percent chord lines and streamwise ribs and from comparison with previously published data on a wing with the same plan form but constructed with spanwise spars and orthogonal streamwise ribs, the following conclusions may be made:

1. At Mach numbers from 0.79 to 0.96 flutter was obtained on both wings, at nearly the same values for each of the parameters, flutter-speed coefficient divided by the square root of the mass-density ratio and the ratio of flutter frequency to torsion frequency.

2. A sharp rise in the parameter flutter-speed coefficient divided by the square root of the mass-density ratio was obtained near Mach number 1.05 for the wing with spanwise spars; the rise in this parameter was associated with a change in flutter mode. Flutter points obtained at subsonic Mach numbers and no-flutter points obtained at supersonic Mach numbers also indicate a sharp rise in the parameter at about the same Mach number for the wing with spars along constant-percent chord lines.

3. Values of the parameter flutter-speed coefficient divided by the square root of the mass-density ratio were about 10 percent higher at a Mach number of about 1.05 for the no-flutter points obtained with the wing with spars along constant-percent chord lines than for the flutter points obtained with the wing with spanwise spars.

Langley Aeronautical Laboratory,
National Advisory Committee for Aeronautics,
Langley Field, Va., June 17, 1957.

REFERENCES

1. Lauten, William T., Jr., and Burgess, Marvin F.: Flutter Investigation in the High Subsonic and Transonic Speed Range on Cantilever Delta-Wing Plan Forms With Leading-Edge Sweepback of 60°, 53°8', and 45°. NACA RM L56K26, 1957.

2. Jones, George W., Jr., and Young, Lou S., Jr.: Transonic Flutter Investigation of Two 64° Delta Wings With Simulated Streamwise Rib and Orthogonal Spar Construction. NACA RM L56I27, 1957.

3. Unangst, John R., and Jones, George W., Jr.: Some Effects of Sweep and Aspect Ratio on the Transonic Flutter Characteristics of a Series of Thin Cantilever Wings Having a Taper Ratio of 0.6. NACA RM L55I13a, 1956.

4. Bursnall, William J.: Initial Flutter Tests in the Langley Transonic Blowdown Tunnel and Comparison With Free-Flight Flutter Results. NACA RM L52K14, 1953.

5. Herr, Robert W.: A Preliminary Wind-Tunnel Investigation of Flutter Characteristics of Delta Wings. NACA RM L52B14a, 1952.

TABLE I.- PHYSICAL PARAMETERS

(a) Wing properties

Parameter	Test wing
Λ, deg	64
Span, ft	1.092
Panel span, ft	0.421
b_r, ft	0.2422
x_{cg}, avg	0.486
g_h, avg	0.0116
ω_1/ω_3	0.2740
ω_2/ω_3	0.6256
Exposed panel mass, slugs	0.00366
f_1, cps	120
f_2, cps	274
f_3, cps	438

(b) Measured mass properties

Strip	$m\delta$, slugs	$I_\alpha\delta$, slug-ft^2	x_{cg}	δ, ft	b, ft
1	0.001672	0.00009557	0.4855	0.0833	0.416
2	0.0009210	0.00003176	0.4875	0.0833	0.331
3	0.0005852	0.00001153	0.4832	0.0833	0.245
4	0.0003091	0.00000300	0.470	0.0833	0.159
5	0.0001720	0.00000043	0.503	0.0875	0.0512

[redacted]

TABLE II.- COMPILATION OF RESULTS

Run	Point	Wing behavior (a)	ρ_e, slugs/cu ft	f_α, cps	f_e, cps	$\frac{\omega_e}{\omega_\alpha}$	V_e, ft/sec	μ_e	M_e	q_e, lb/sq ft	$\frac{V_e}{b_r\omega_\alpha\sqrt{\mu_e}}$	$\frac{V_e}{b_r\omega_\alpha}$	$\frac{b_r\omega_e}{V_e}$
1	1	D	0.0028	438	---	------	835.2	16.84	0.782	979	0.3052	1.2525	------
	2	F	.0029	438	197	0.4498	882.2	16.26	.832	1129	.3281	1.3230	0.3400
2	1	F	.0047	438	241	.5502	744.5	10.03	.693	1297	.3525	1.1165	.4927
3	1	F	.0028	438	217	.4954	935.4	16.84	.892	1227	.3418	1.4028	.3531
4	1	F	.0030	438	243	.5548	863.4	15.72	.815	1138	.3266	1.2948	.4285
5	1	D	.0041	438	---	-----	783.6	11.50	.735	1274	.3465	1.1751	------
	2	F	.0046	438	230	.5251	783.6	10.25	.739	1416	.3670	1.1751	.4468
6	1	F	.0036	438	233	.5320	829.0	13.10	.785	1251	.3435	1.2432	.4279
7	1	D	.0033	438	---	------	854.7	14.29	.800	1194	.3391	1.2818	------
	2	F	.0036	438	250	.5708	867.9	13.10	.819	1349	.3596	1.3016	.4386
8	1	F	.0028	438	220	.5023	904.7	16.84	.849	1152	.3306	1.3568	.3701
9	1	D	.0036	438	---	------	833.3	13.10	.779	1264	.3453	1.2497	------
	2	F	.0042	438	233	.5320	822.5	11.22	.773	1418	.3682	1.2335	.4313
10	1	F	.0027	438	233	.5320	966.4	17.46	.923	1259	.3469	1.4493	.3671
	2	E	.0027	438	200	.4566	987.3	17.46	.947	1325	.3544	1.4806	.3085
11	1	D	.0042	438	---	------	783.1	11.22	.735	1305	.3506	1.1744	------
	2	F	.0046	438	225	.5137	771.5	10.25	.724	1377	.3613	1.1570	.4441
12	1	D	.0027	438	---	------	897.4	17.46	.849	1104	.3221	1.3458	------
	2	F	.0028	438	216	.4940	931.3	16.84	.887	1217	.3403	1.3966	.3530
	3	E	.0030	438	233	.5320	992.9	15.72	.958	1475	.3755	1.4890	.3573
13	1	Q	.0071	438	---	------	1012.8	6.64	1.055	3640	.5894	1.5189	------
14	1	Q	.0058	438	---	------	1191.0	8.13	1.314	4159	.6265	1.7861	------
15	1	Q	.0070	438	---	------	1047.2	6.73	1.105	3833	.6052	1.5705	------

[a]Wing panel behavior code:

F - flutter
E - end of flutter (dynamic pressure increasing)
D - low damping
Q - maximum dynamic pressure, no flutter

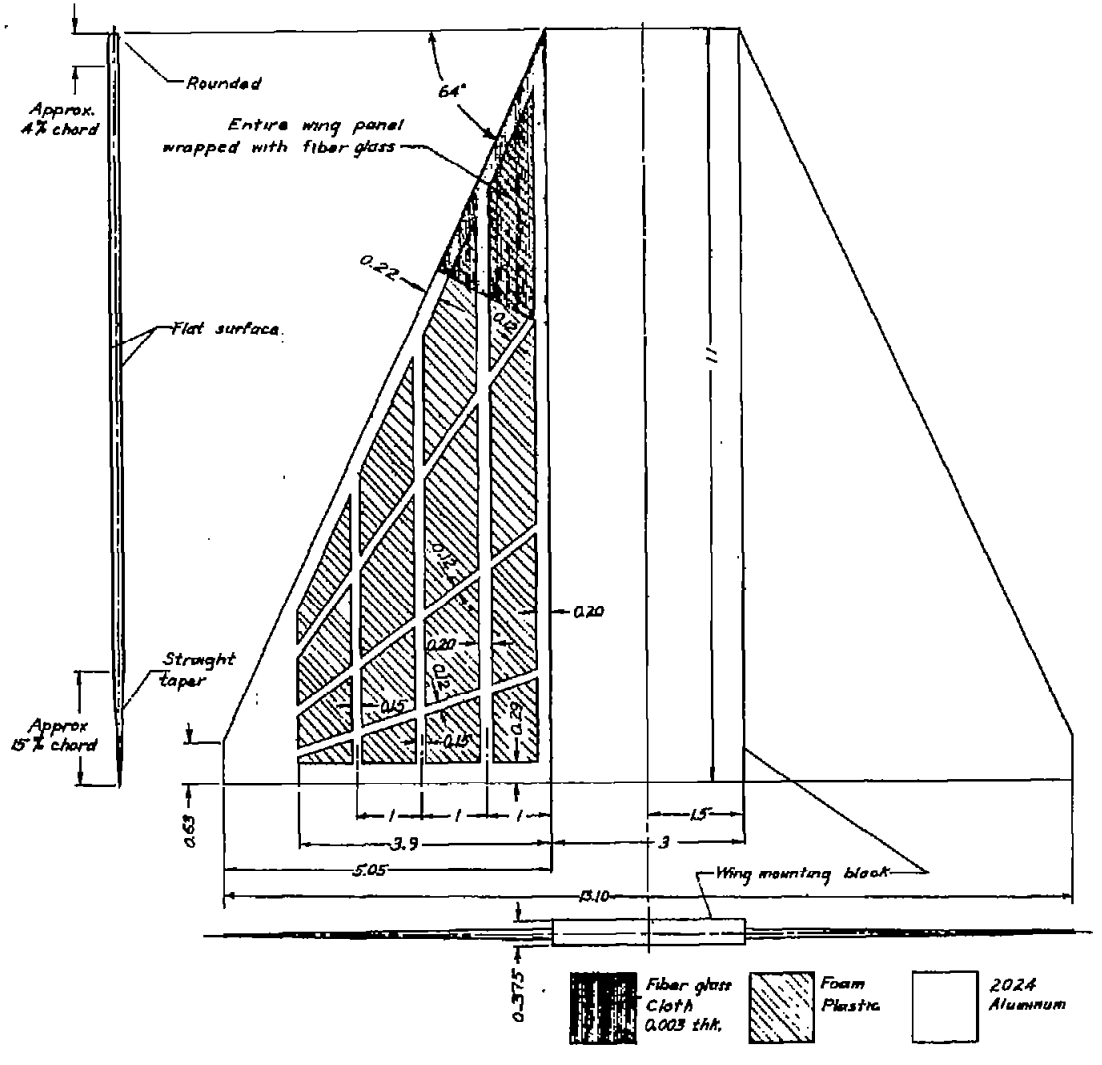

Figure 1.- Sketch of wing showing basic dimensions and construction. Forward spar, 0.35 chord; middle spar, 0.65 chord; and rear spar, 0.85 chord. All dimensions are in inches.

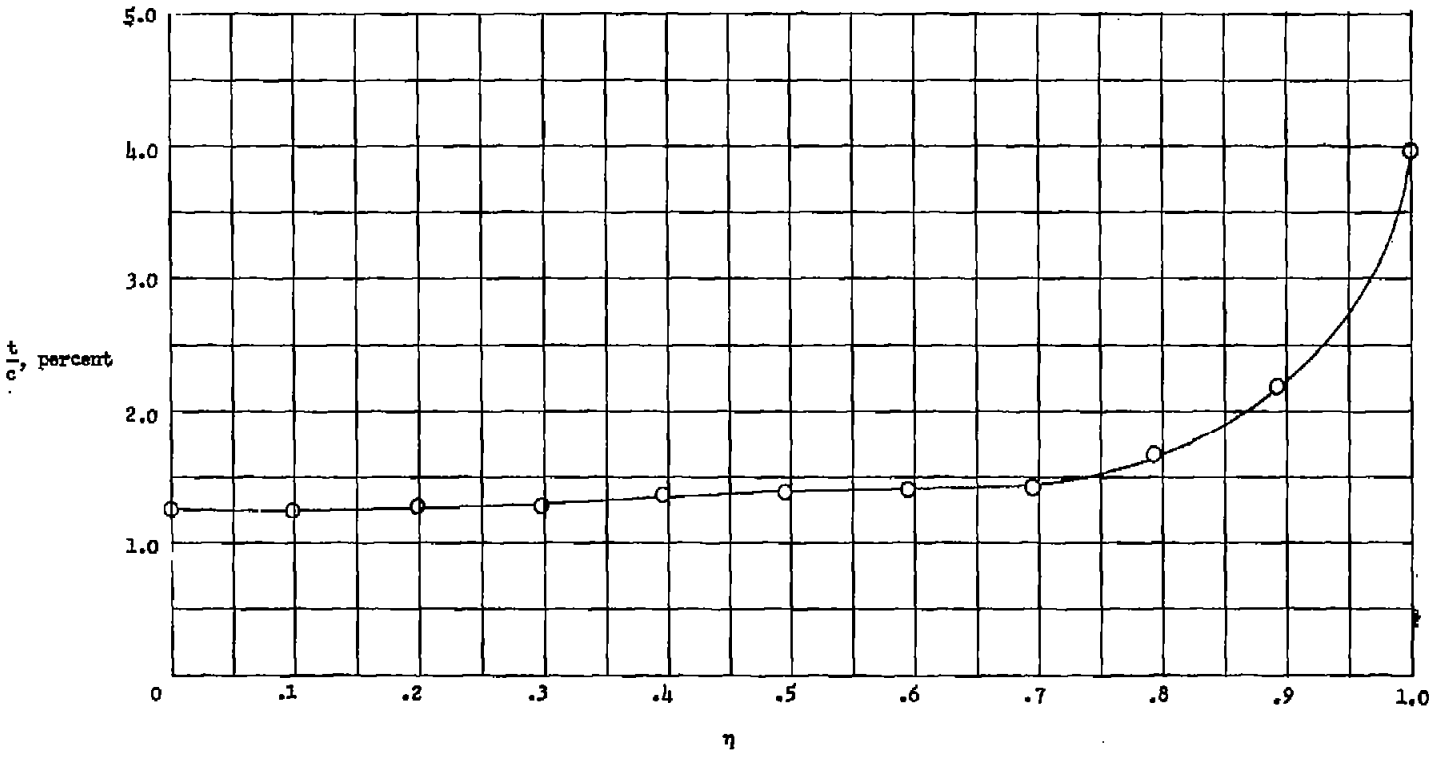

Figure 2.- Variation of test wing ratio of average thickness (over flat part of wing) to streamwise chord along the wing span.

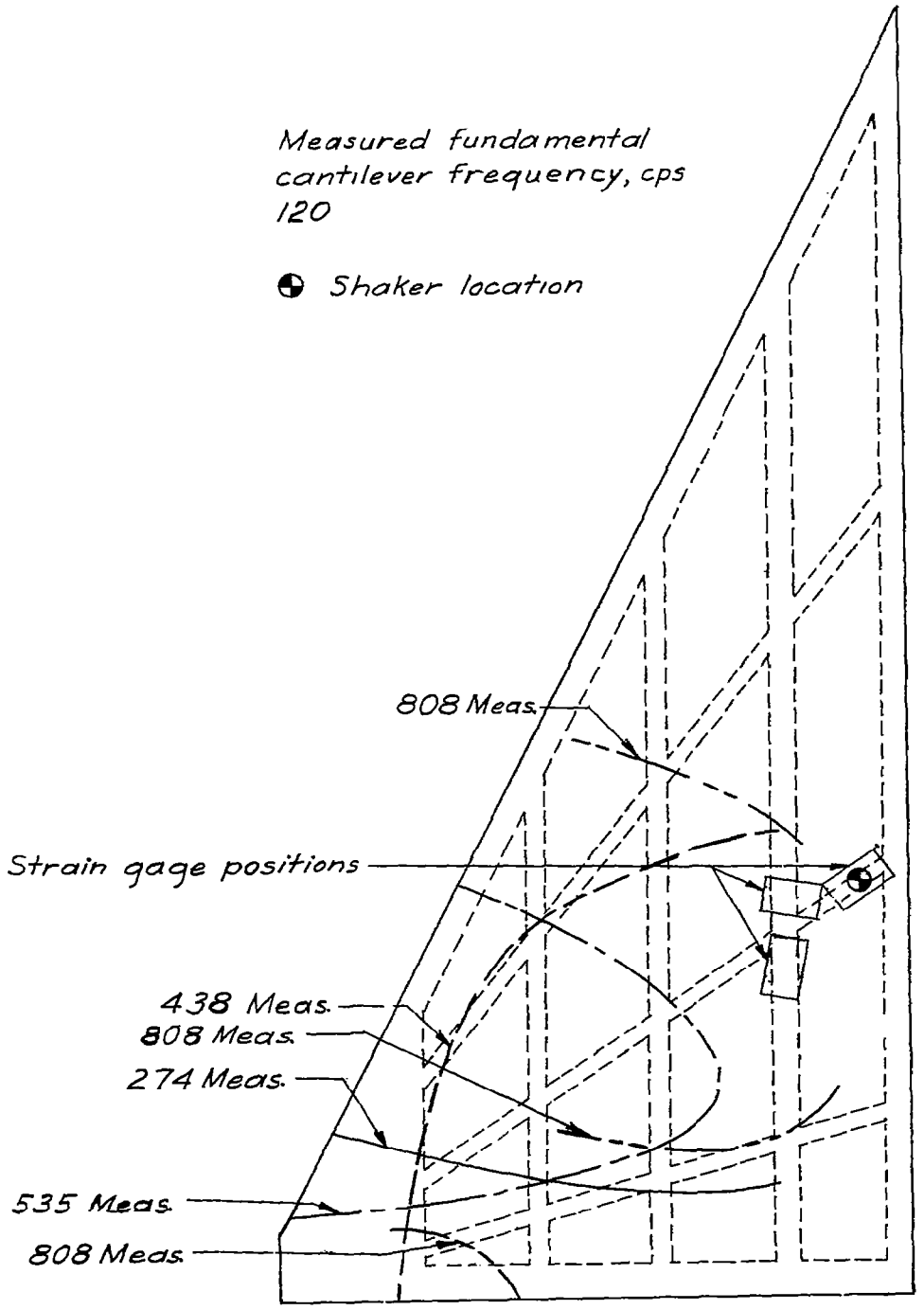

Figure 3.- Measured coupled natural vibration frequencies and node lines, shaker position, and strain-gage locations for test wing.

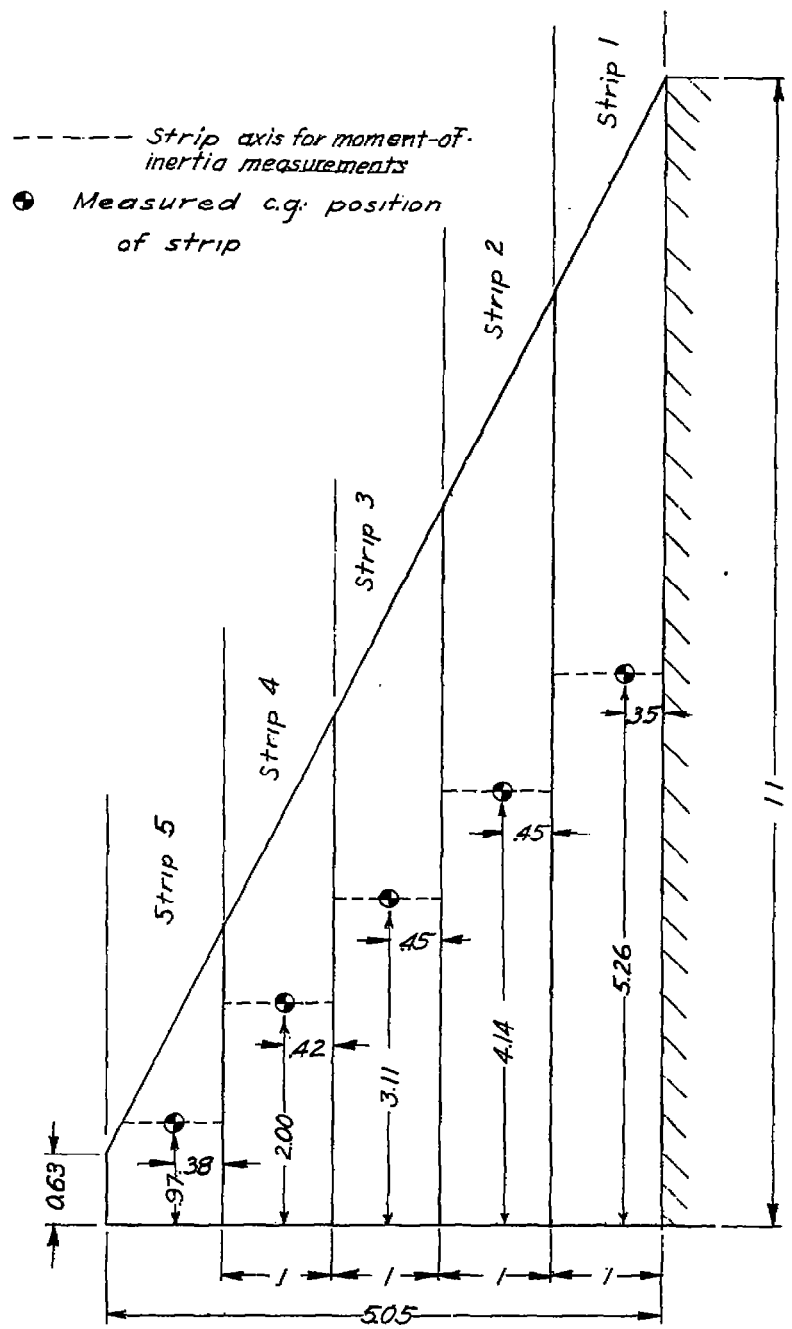

Figure 4.- Sketch of test wing showing streamwise strips, strip center-of-gravity locations, and assumed strip axes for moment-of-inertia measurements. All dimensions are in inches.

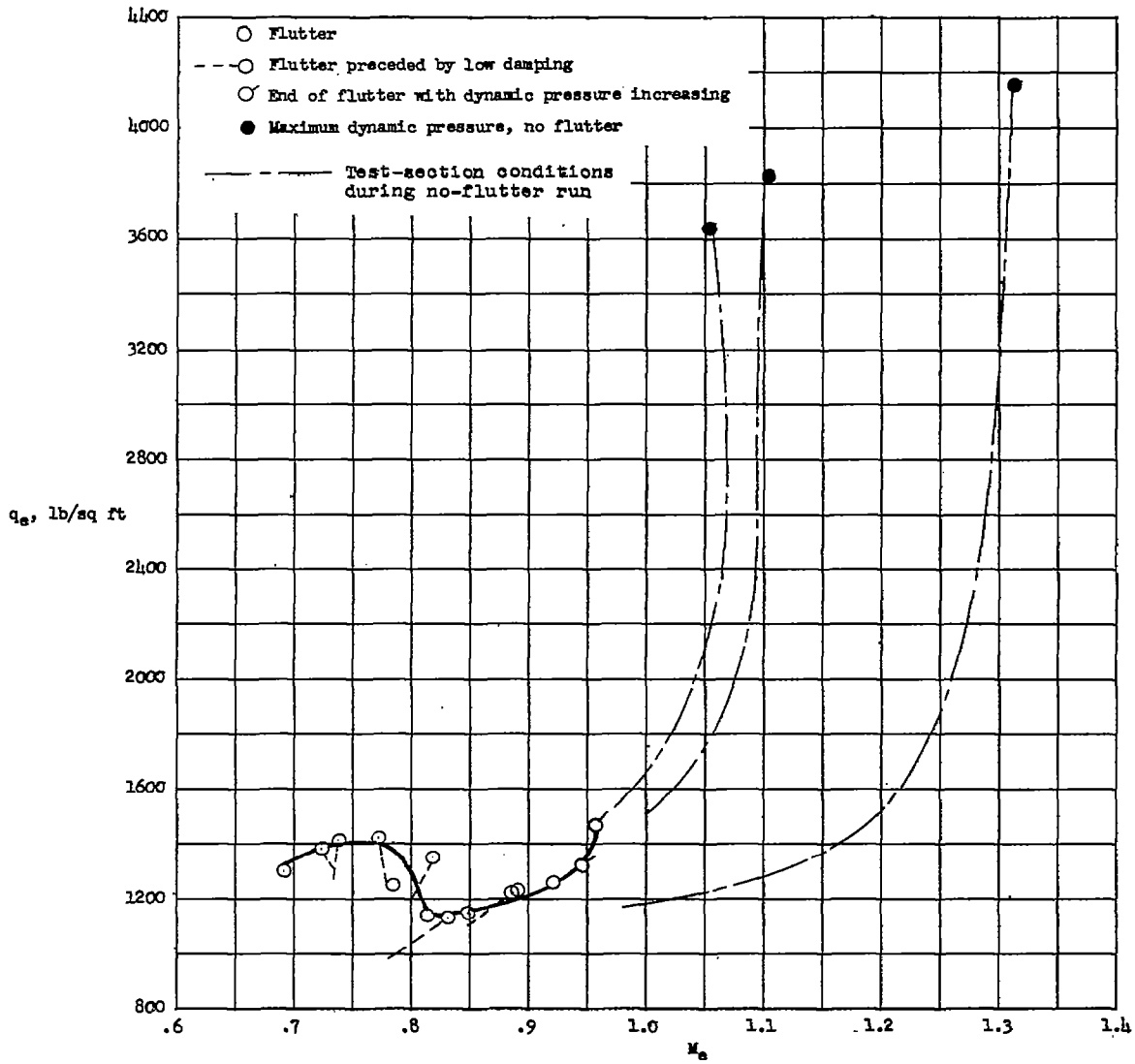

Figure 5.- Variation for test wing of free-stream dynamic pressure at flutter with Mach number.

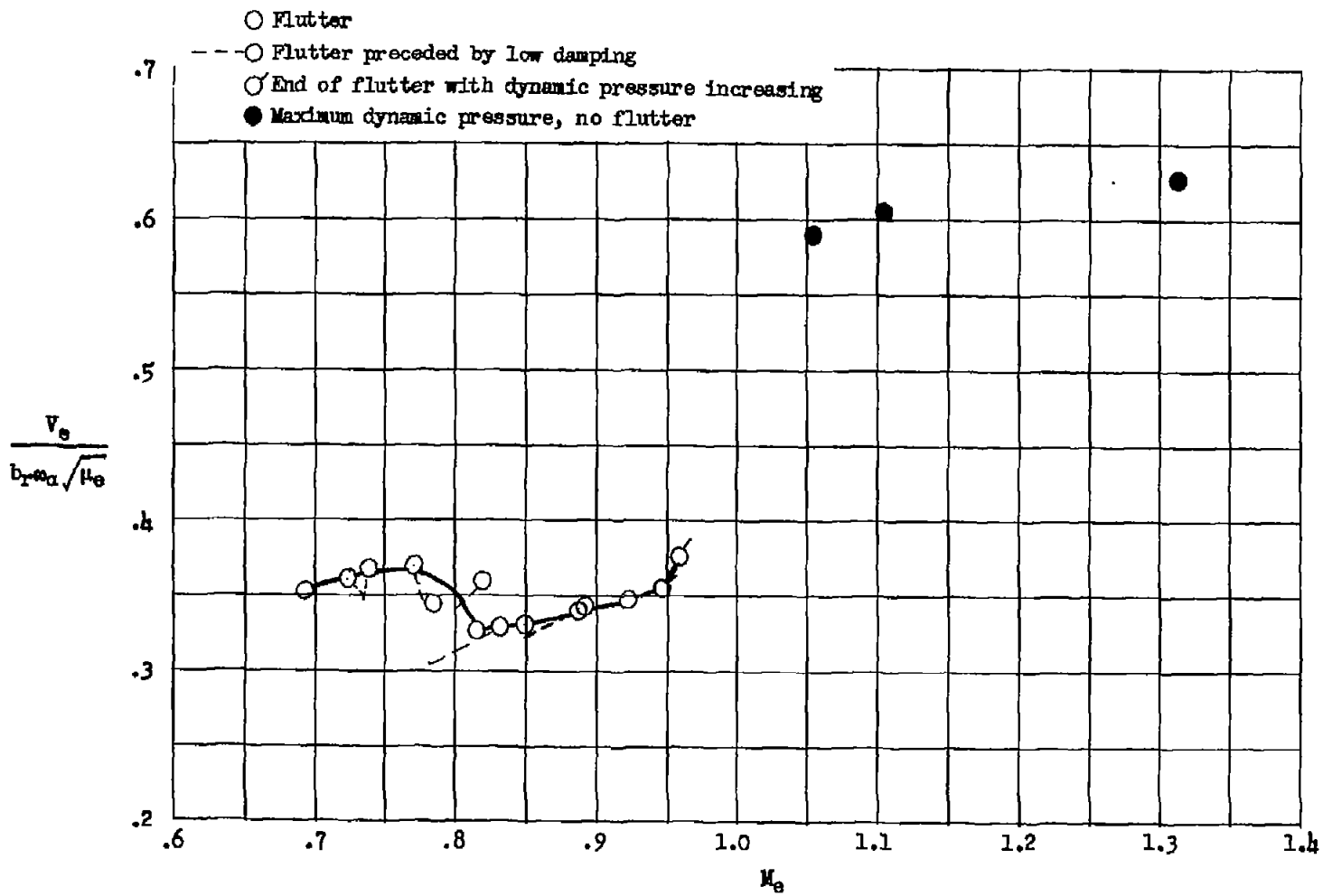

Figure 6.- Variation for test wing of the parameter $\frac{V_e}{b_r \omega_\alpha \sqrt{\mu_e}}$ with Mach number.

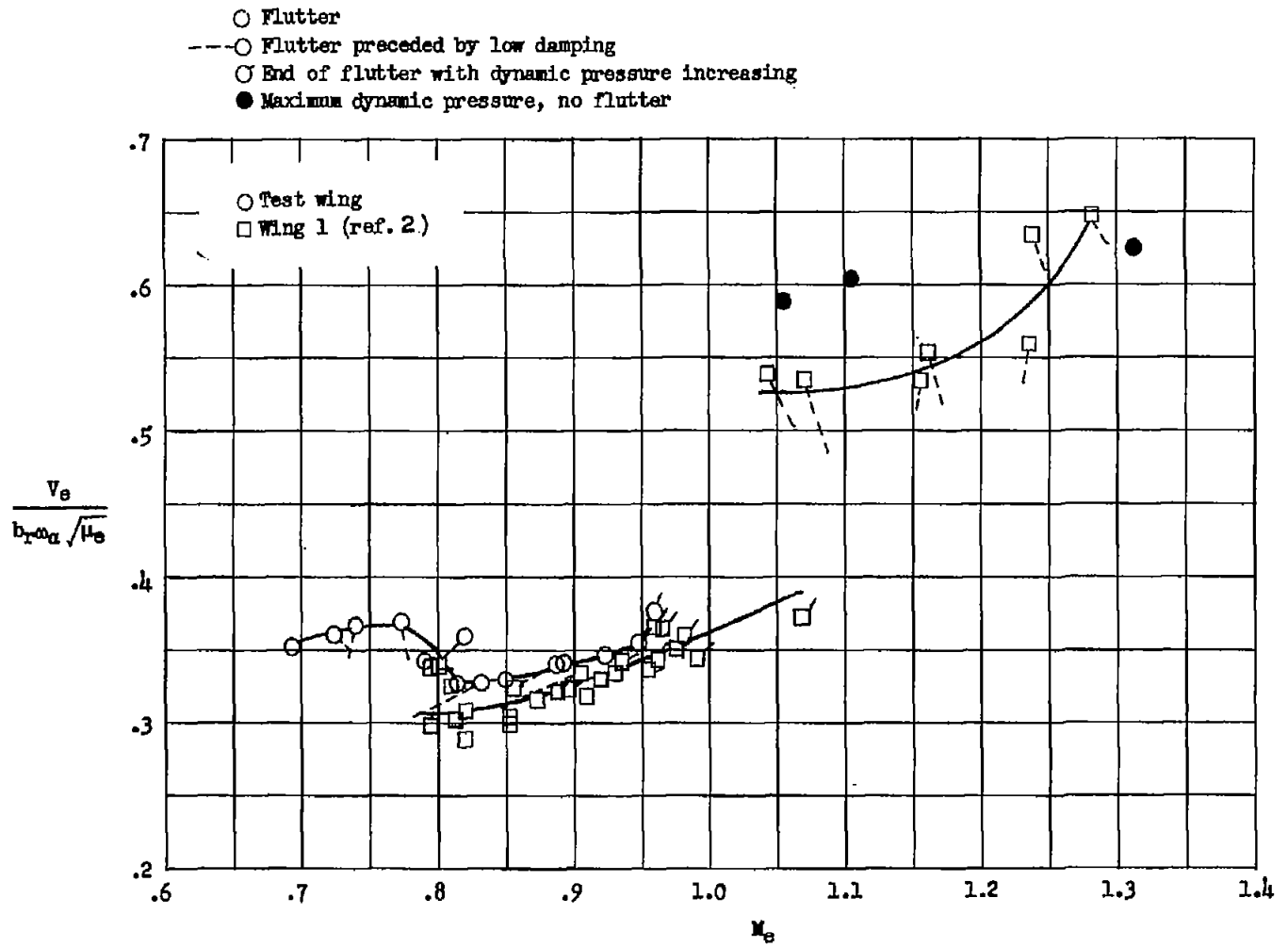

Figure 7.- Comparison of values of $\frac{V_e}{b_r \omega_\alpha \sqrt{\mu_e}}$ as a function of Mach number for test wing with values of same parameter for wing 1 of reference 2.

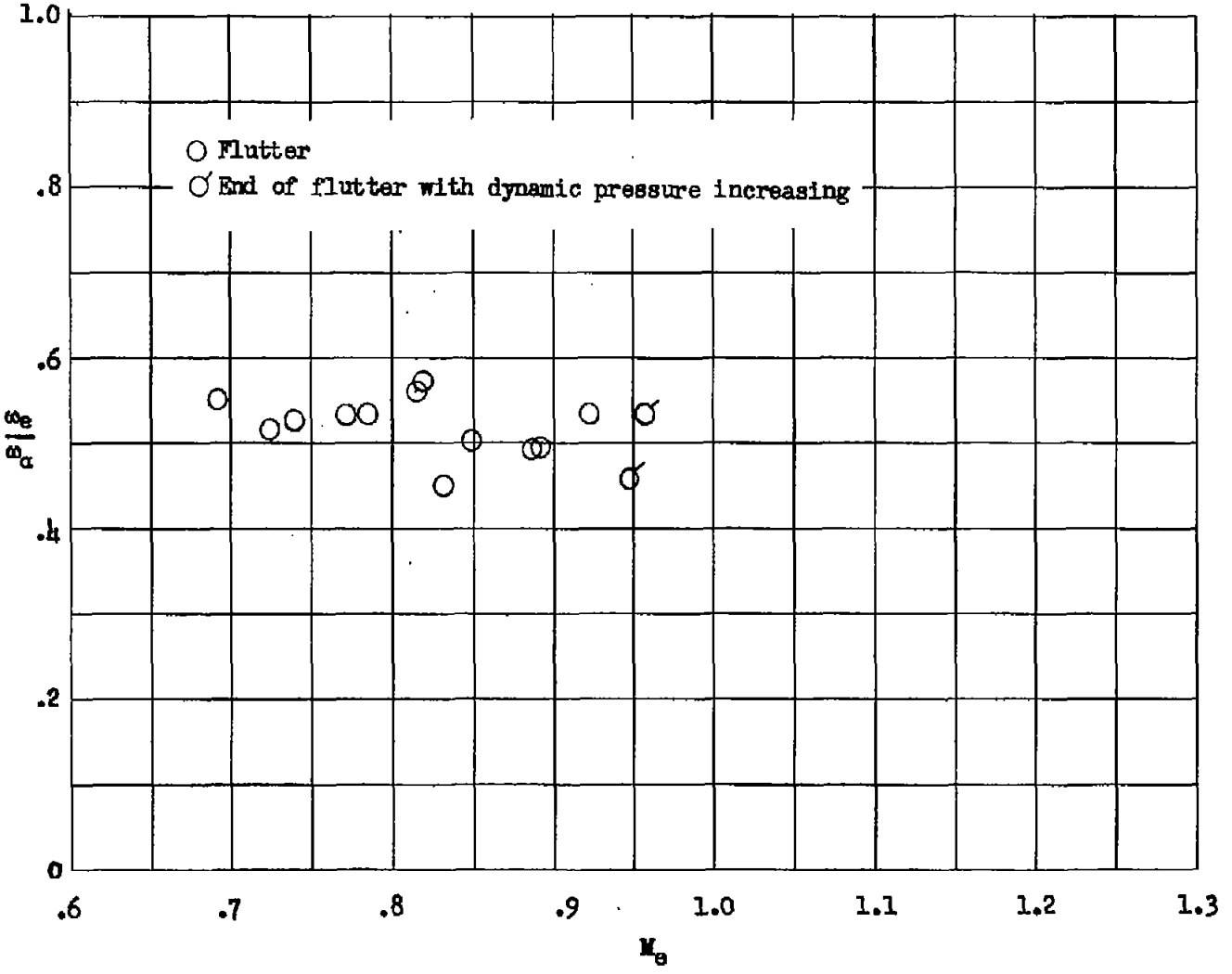

Figure 8.- Variation of ratio of flutter frequency to measured predominantly torsion frequency with Mach number for test wing.